Available online at www.sciencedirect.com
ScienceDirect
Vibrational Spectroscopy 41 (2006) 190–197
VIBRATIONAL SPECTROSCOPY
www.elsevier.com/locate/vibspec

Raman spectroscopy reveals thermal palaeoenvironments of c.3.5 billion-year-old organic matter

Abigail C. Allwood [a], Malcolm R. Walter [a], Craig P. Marshall [b,*]

[a] *Australian Centre for Astrobiology, Department of Earth and Planetary Sciences, Macquarie University, Herring Rd, Sydney, NSW 2109, Australia*
[b] *Vibrational Spectroscopy Facility, School of Chemistry, The University of Sydney, NSW 2006, Australia*

Received 29 October 2005; received in revised form 21 January 2006; accepted 3 February 2006
Available online 5 April 2006

Abstract

Raman spectra of carbonaceous materials in one of the world's oldest sedimentary rock formations – the Strelley Pool Chert (Pilbara Craton, Western Australia) – are analysed to determine whether primary structural characteristics of organic molecules may have survived to the present day. We use Raman spectral parameters to identify variations in molecular structure of the carbon and determine whether original characteristics of the carbonaceous materials have been completely thermally overprinted, as would be expected during c.3.5 billion years of geologic history. To the contrary, we find that the molecular structure of the carbonaceous materials varies depending on the sedimentary layer from which the sample came and the inferred original palaeoenvironmental setting of that layer, as determined by other geochemical and geological data. Thus, we argue that the spectral characteristics of the carbonaceous materials reflect original palaeoenvironments that varied through time from warm hydrothermal settings to cooler marine conditions and a return to hydrothermal conditions. Raman spectroscopy is also used to show that organic matter is present in trace amounts in association with putative stromatolites (laminated sedimentary structures possibly formed by microorganisms) in the Strelley Pool Chert, which were previously thought to be devoid of organic remains. Furthermore, the Raman spectra of carbon associated with stromatolites indicate lower thermal maturity compared to the carbon in (non-stromatolitic) hydrothermal deposits above (younger) and below (older). Significantly, this indicates that the stromatolites are not abiotic hydrothermal precipitates – as previously proposed – but were formed in a cooler marine environment that may have been more favorable to life.

Keywords: Raman spectroscopy; Carbonaceous materials; Palaeoenvironments; Archaean; Pilbara; Strelley Pool Chert

1. Introduction and background

Examining remnants of organic material in Earth's oldest sedimentary rocks is an essential part of tracing the origins of life on our planet and is important for developing techniques to search for traces of life on other planets. Accordingly, carbonaceous materials (CM) in Early Archaean age (3.2–3.5 billion-year-old) sedimentary rocks are coming under scrutiny to determine whether evidence of biology can be elucidated from their physical and chemical characteristics. Raman spectroscopy is emerging as a useful tool in that research by enabling simple, in situ, non-destructive evaluation of CM in geological samples. Raman spectroscopy has been used to demonstrate a carbonaceous composition for putative microfossils in Early Archaean age rocks [1]. In some cases, Raman has been used to infer a biological [2] origin of putative microfossils. In other cases, Raman spectra have been cited as evidence of a non-biological origin for microfossils [3]. However, studies have shown that non-biological and biological CM display similar Raman spectral properties [4]. This is because thermal maturation or metamorphism processes that affect rocks during burial can be expected to produce essentially the same set of thermally stable carbonaceous products (interlinked polyaromatic hydrocarbons, or PAHs) for almost all naturally occurring organic matter, whether biological or abiological in origin. Therefore, Raman spectroscopy of metamorphosed CM cannot, by itself, provide definitive evidence of biogenicity [5]. Nonetheless, Raman spectroscopy can do more than simply demonstrate a carbonaceous composition for trace materials in rock: it can also reveal macromolecular structural characteristics that may provide important constraints on the origin and history of the

* Corresponding author. Tel.: +61 2 9351 3994; fax: +61 2 9351 3329.
E-mail address: c.marshall@chem.usyd.edu.au (C.P. Marshall).

0924-2031/$ – see front matter
doi:10.1016/j.vibspec.2006.02.006

carbon. Moreover, it can potentially give insights to the palaeoenvironment in which the carbon was deposited, which is an essential step toward establishing whether any of the CM may contain primary molecular information—particularly biomarker molecules that indicate a biological origin.

Here we use Raman spectroscopy to study in situ CM in thin section from different beds and depositional facies of a 3.43 billion-year-old sedimentary rock formation called the Strelley Pool Chert, which is widely exposed across the 220 km-wide Pilbara Craton of Western Australia [6]. The Strelley Pool Chert is a ~30 m-thick sedimentary succession containing putative fossil stromatolites (laminated sedimentary structures formed by microbes) in carbonate beds and abundant CM in black chert beds. We use Raman spectroscopy to study the structural organization (degree of carbonization/graphitization) in the carbonaceous macromolecular network and investigate – in particular – the level of thermal treatment that different CM in the Strelley Pool Chert has undergone during a 3.43 billion-year history.

2. Samples

The samples analysed in the present study were collected from surface outcrops of the Strelley Pool Chert in the southwest North Pole Dome in the Pilbara Craton of Western Australia (Fig. 1). The sample locality has exceptionally low degrees of alteration compared to most outcrops of the formation. The locality has good exposures of primary sedimentary carbonate rocks – with putative stromatolites – as well as a range of black cherts of different primary sedimentary and intrusive origin (i.e., hydrothermal veins). The bedded and vein chert rocks consist of microcrystalline quartz with some larger grained quartz (megaquartz). The carbonate rocks are more complex, containing finely interlaminated dolomite ([Fe/Mg/Ca]CO_3) and chert (microcrystalline quartz). A variety of stromatolite forms occur in the area, each consisting of laminated dolomite and chert stacked in successive domed, crested, conical or other shaped layers to form pseudocolumns up to 1.2 m high (exposed in cross-section) [7–12]. Because the samples were collected from one locality, it is likely that all have undergone similar post-depositional burial (and thermal) history.

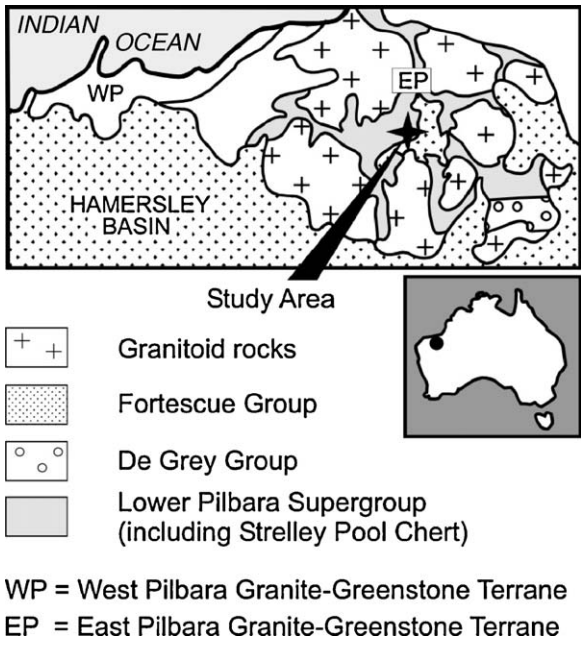

Fig. 1. Location map showing the study area in the North Pole Dome, East Pilbara granite-greenstone terrane, Western Australia.

The geologic context of the sampled rocks was documented on a detailed stratigraphic column (reconstructed succession of deposited sediments; Fig. 2). At the sample locality the Strelley Pool Chert is divided into four major sub-units (Members 1–4) [9–12], which were deposited on a regional erosion surface over older, metamorphosed volcanic and sedimentary rocks [6,13,14]. The following samples were analysed: (1) black chert beds in the older, underlying volcanic/sedimentary beds; (2) Black chert pebbles from Member 1 (a rocky coastal conglomerate); (3) black chert beds in Member 3 (a mixed hydrothermal/shallow marine deposit); (4) black chert beds and black chert veins of Member 4 (a deposit of clastic, volcanic and hydrothermal sediments); (5) laminated stromatolitic carbonate samples in Member 2 (a peritidal marine carbonate platform deposit) [7–12]. The stromatolite samples are from conical structures and laminated structures that encrust boulders of the underlying Member 1 conglomerate. The samples were prepared as 30 μm-thick, glass slide-mounted polished sections of rock, which were examined under a microscope before Raman spectroscopic analysis.

3. Experimental

Raman spectra were collected on the black clots and clasts seen in thin section. It is preferable to study these materials in thin section rather than bulk powders because natural CM are generally disordered, but more importantly, are structurally, microtexturally, and texturally heterogeneous. Furthermore, graphite and other CM have strong structural anisotropy and thus do not exhibit the same Raman spectrum when the measurement is performed parallel or perpendicular to the *c*-axis [15–18]. The fine scale variability within the sample is assessed by studying the materials in thin section, recording spectra from multiple points in each sample to check the consistency of the spectral characteristics. Care was also taken to target dense black material that is part of the primary rock fabric, avoiding material in cross-cutting (younger) veins.

The Raman spectra were acquired on a Renishaw Raman Microprobe Laser Raman Spectrometer using a charge-coupled detector. The collection optics are based on a Leica DMLM microscope. A refractive glass 50× objective lens was used to focus the laser onto a 2 μm spot to collect the backscattered radiation. The 514.5 nm line of a 5 W Ar^+ laser (Spectra-Physics Stabilite 2017 laser) orientated normal to the sample was used to excite the sample. The instrument was calibrated against the Raman signal of Si at 520 cm^{-1} using a silicon wafer (1 1 1). Surface laser powers of 1.0–1.5 mW were used to

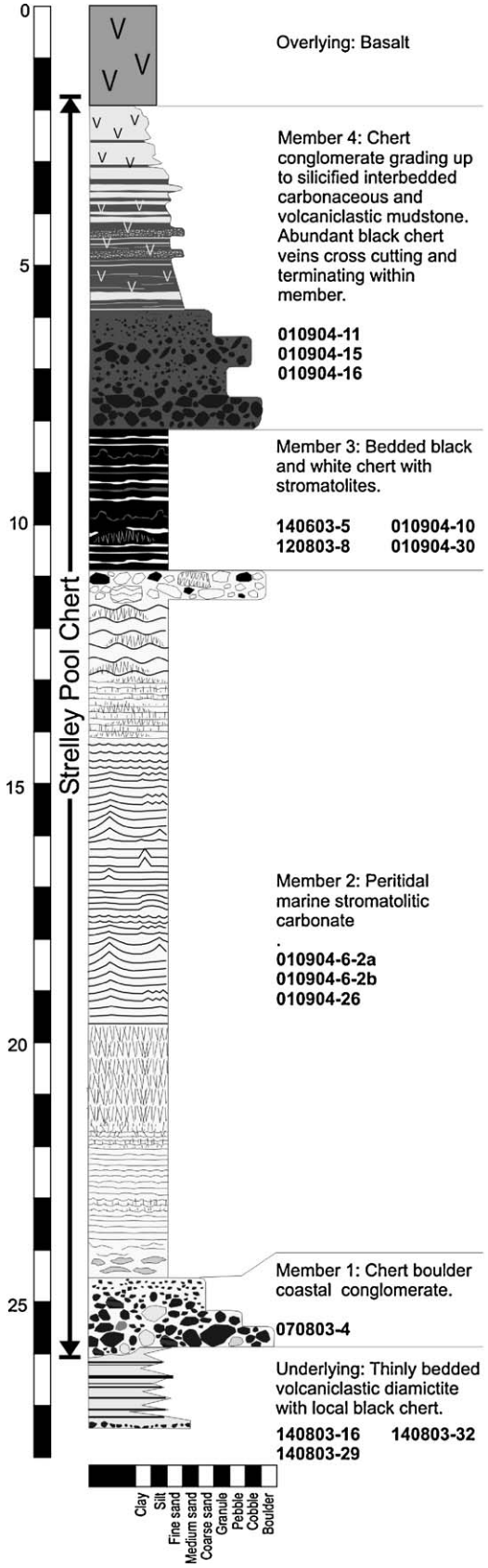

Fig. 2. Stratigraphic column of the Strelley Pool Chert at the sample location, showing the four sub-members, underlying and overlying rocks. Bold sample numbers at right show stratigraphic location of each sample, with description of the palaeoenvironment in which the sediments were originally deposited.

minimize laser induced heating of the CM. The laser induced heating can be easily detected as it is responsible for a shifting of the G band position downward to 1565 cm^{-1}. There was no G band position shift downward to 1565 cm^{-1} observed for any spectra acquired in this study. Each spectrum was acquired using 10 scans and an accumulation time of 30 s, which gave good signal-to-noise ratio. The scan ranges were 1000–1800 cm^{-1} in the carbon first-order region.

The spectra were deconvoluted with a Gaussian/Lorentzian fit routine using GRAMS/32 software in order to follow small spectroscopic changes with accuracy. The parameters were fitted to the experimental envelope by a least squares iterative procedure. In order to determine the goodness of fit criteria the following aspects were considered: (1) standard errors of parameters (χ-squared), (2) local poor fits (indicative of an incorrect choice of the number of component peaks or errors in their half-widths), and (3) the degree of coincidence of the second derivative (original and fitted spectrum).

4. Results and discussion

The CM in chert samples consist of clots or clasts of black material finely disseminated through a matrix of polygonal microcrystalline quartz. The samples also contain variable quantities of silicified rock and mineral grains (Fig. 3). In samples from bedded cherts, the carbonaceous clots and clasts, together with the other grains, define a laminated rock fabric (Fig. 3a) that is concordant with primary bedding and sedimentary fabrics observed in outcrop and across the area. This indicates that the carbon was deposited as part of the original sediment and is not a younger contaminant. CM in sample 010904–11 (from a black chert vein in Member 4) occur as sub-millimetre-sized ragged grains and clots arranged in a massive (non-laminated) fabric. CM in samples 010904-6-2a, 010904-6-2b and 010904-26 occur as rare, thin wisps concordant with chert-carbonate laminae: each wisp contains ragged clots of CM. CM in the black chert pebbles from Member 1 occurs as sub-millimetre-sized grains and clots that define laminae (including graded laminae) in the pebbles. This indicates that the CM in the pebbles had a transport history prior to the formation and transport of the pebbles.

Raman spectra of black materials in the Strelley Pool Chert samples are presented in Fig. 4. The main spectral features between ~900 and 1800 cm^{-1} are two distinct bands at approximately 1350 cm^{-1} and 1600 cm^{-1}. In addition, there are less intense features at ~1200 cm^{-1} and 1620 cm^{-1} – visible as shoulders on the main bands – and high signal intensity between the main bands. These combined spectral features represent the first-order bands of disordered sp^2 carbons.

For an ideal graphite crystal (space group D^4_{6h} with unlimited translational symmetry) only one first-order band-the G (Graphite) band-is exhibited at 1580 cm^{-1}. The G band corresponds to an ideal graphitic lattice vibrational mode with E_{2g} symmetry [19]. Disordered CM such as in the Strelley Pool Chert, on the other hand, also display D or defect bands characteristic of disordered sp^2 carbons. The D bands, which decrease in intensity relative to the G band as further order is

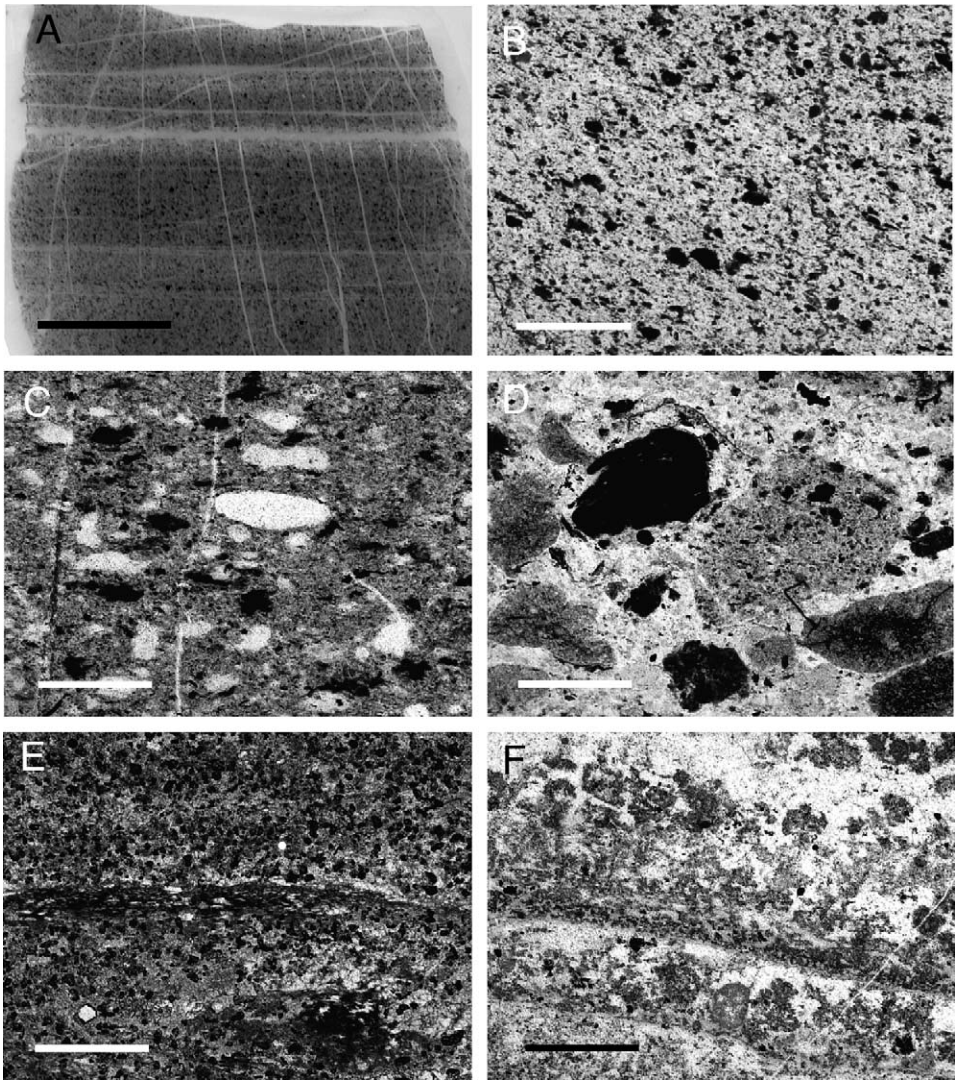

Fig. 3. Thin section photomicrographs showing variety of textures of carbonaceous materials in the Strelley Pool Chert. (A) Sample 120803-8: laminated fabric is defined by size variations of sub-millimetre-sized carbonaceous grains in a transparent chert matrix. Scale bar = 0.5 cm. (B) 120803-8 in plane-polarized light (PPL). (C) 140803–32: carbonaceous clasts and clots distributed among rounded transparent chert grains (PPL). (D) 010904–15: carbonaceous grains (PPL). (E) 140603–5 carbonaceous clots and grains chert matrix (PPL). (F) 140803–16 carbonaceous material with clotted fabric (PPL). Scale bar in (B)–(F) = 0.5 mm.

introduced into the graphitic structure (i.e., through metamorphism), are as follows:

- D1—1350 cm^{-1}: The most intense D band, corresponding to a disordered graphitic lattice vibration mode with A_{1g} symmetry. This vibration mode has been suggested to arise from graphene layer carbon atoms in immediate vicinity of a lattice disturbance such as the edge of a graphene layer [16], or a heteroatom [15].
- D2—1620 cm^{-1}: Observed as a shoulder on the G band, corresponding to a graphitic lattice mode with E_{2g} symmetry. The D2 band is assigned to a lattice vibration involving graphene layers at the surface of a graphite crystal [20]. The relative intensities of both the D1 and D2 bands increase with increasing excitation wavelength, which can be attributed to resonance effects [21]. The D2 shoulder becomes more pronounced with increasing disorder, producing an apparent broadening and up-shifting of the G band. [22–24] and gradual merging of the G and D2 bands merge until a single feature is observed around 1600 cm^{-1}.
- D3—1550 cm^{-1}: Assigned to amorphous carbon fraction of organic molecules, fragments or functional groups [24,25].
- D4—1200 cm^{-1}: Observed as a shoulder on the D1 band. Tentatively attributed to sp^2–sp^3 bonds or C–C and C=C stretching vibrations of polyene-like structures. These polyene C–C=C–C structures are bridging units that link the aromatic domains [19,26].

Thus, the 1600 cm^{-1} band in the Strelley Pool Chert sample spectra is attributed to a combination of the D2 (1620 cm^{-1}) and G (1580 cm^{-1}) bands. The band at 1350 cm^{-1} is assigned to D1, with the shoulder assigned to the D4 band at 1200 cm^{-1}, and the region of high intensity between the G and D1 band is assigned to the D3 band (~1550 cm^{-1}). A representative deconvoluted spectrum of CM in the Strelley Pool Chert samples shows the G, D1, D3 and D4 bands (Fig. 5).

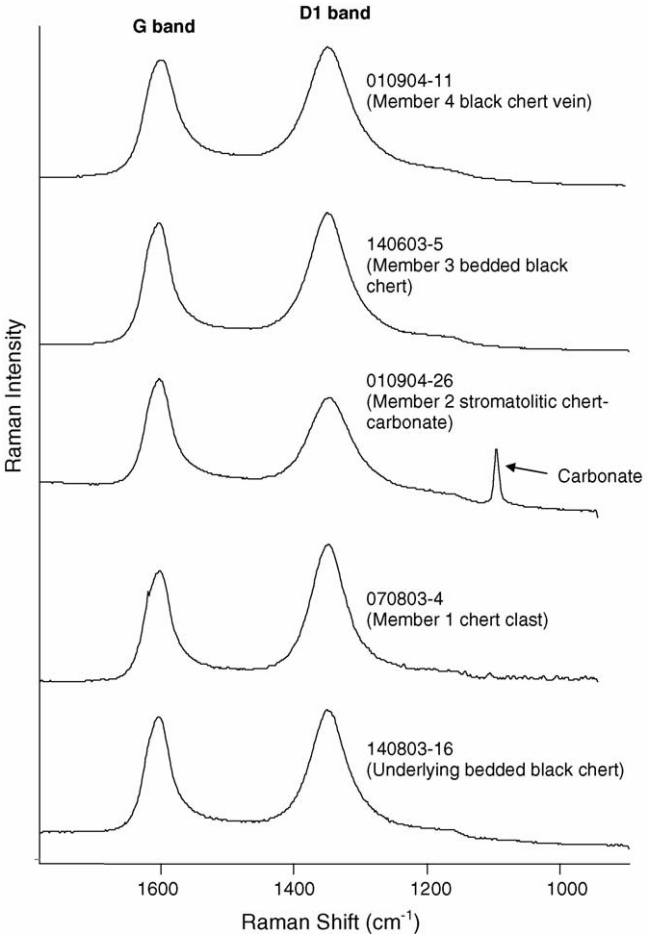

Fig. 4. Representative Raman spectra of a sample from each Member of the Strelley Pool Chert and underlying rocks. Note that the D band is more intense than the G band in samples from Member 1, 3, 4 and underlying rocks, whereas it is less intense in Member 3.

The thermal maturity of the CM can be examined by determining the width of the G band (full-width at half-maximum, or G_{FWHM}) and the relative intensity of the G and D bands (I_{D1}/I_G and $I_{D1}/\{I_{D1} + I_G\}$) on the deconvoluted spectra.

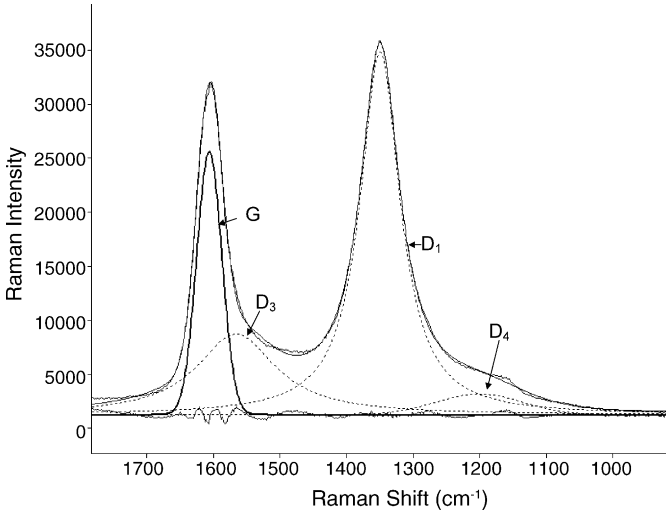

Fig. 5. Representative deconvoluted Raman spectrum (sample 140803–16), showing the overlapping G/D_3 bands (D_2 not resolved in this sample), and D_1/D_4 bands.

Those parameters have been shown to correlate with the amount of structural disorder in the CM and may be considered as an index of thermal treatment or metamorphic alteration [27,24 and references therein].

Broadly, the spectra of our samples indicate that CM in the Strelley Pool Chert has a low degree of two-dimensional structural organization, and the spectral characteristics of the G and D bands in most samples are comparable with spectra of other CM taken from chlorite up to biotite grade metamorphic rocks [e.g., 4,28 and references therein]. This represents lower to mid Greenschist metamorphic facies [29] or peak temperatures from ~300–400 °C through to 400–500 °C [30].

In detail, for CM in the range of thermal maturity of our samples, G_{FWHM} has been shown to decrease with increasing thermal maturity, whereas I_{D1}/I_G and $I_{D1}/(I_{D1} + I_G)$ have been shown to increase [e.g., 4,28]. Small but distinct variations occur in the values of G_{FWHM}, I_{D1}/I_G and $I_{D1}/(I_{D1} + I_G)$ for the

Table 1
Summary of spectral data of samples taken from the Strelley Pool Chert, showing the number of spots analysed on each thin section and the total number of spectra acquired from each thin section

Sample	Member	Number of spots	Number of spectra	G_{FWHM}	I_{D1}/I_G	$I_{D1}/(I_{D1} + I_G)$
010904–11	M4	5	6	43.19	1.42	0.59
010904–15	M4	2	2	40.44	1.22	0.55
010904–16	M4	6	6	42.07	1.14	0.53
140603–5	M3	6	6	43.27	1.43	0.59
120803–8	M3	5	5	40.80	1.18	0.54
010904–10	M3	3	3	42.94	1.27	0.56
010904–30	M3	1	1	44.42	1.28	0.56
010904-6-2a	M2	2	2	49.65	1.00	0.50
010904-6-2b	M2	2	2	46.94	0.84	0.46
010904–26	M2	2	2	46.09	0.72	0.42
070803-4	M1 (clasts)	3	3	38.29	1.23	0.55
140803–16	Underlying	12	14	41.33	1.37	0.58
140803–29	Underlying	1	1	44.08	1.14	0.53
140803–32	Underlying	2	2	43.55	1.22	0.55

A representative spectrum from each thin section was deconvoluted to yield the values for G_{FWHM}, I_{D1}/I_G and $I_{D1}/(I_{D1} + I_G)$.

deconvoluted spectra of the Strelley Pool Chert samples (Table 1). Significantly, those variations define a trend of thermal treatment, with samples from Member 3, Member 4 and underlying black cherts tending toward higher thermal maturity and samples from Member 2 showing lower thermal maturity (Fig. 6). The origin of the trend becomes apparent when considered within stratigraphic and palaeoenvironmental context: CM with the greatest structural order (having been subjected to higher maximum temperatures during their history) occur in strata that show geological and geochemical indications of deposition in hydrothermally influenced environments, including hydrothermal veins (Member 3, Member 4 and underlying rocks). In contrast, the CM with the least structural order (indicating those rocks were subjected to lower maximum temperatures) occur in stromatolitic carbonates of Member 2—which were deposited in a peritidal marine environment [7–12].

The occurrence of different thermal signatures in distinct stratigraphic units and facies that represent different palaeoenvironments strongly suggests that the signatures were determined by the surface or near-surface temperatures that prevailed as the carbonaceous sediments were being deposited, rather than a later regional thermal overprint. Arguably, stratigraphic permeability differences could control post-depositional thermal alteration by allowing or impeding the passage of hot fluids. However, additional observations support the former hypothesis. Notably, one of the most thermally

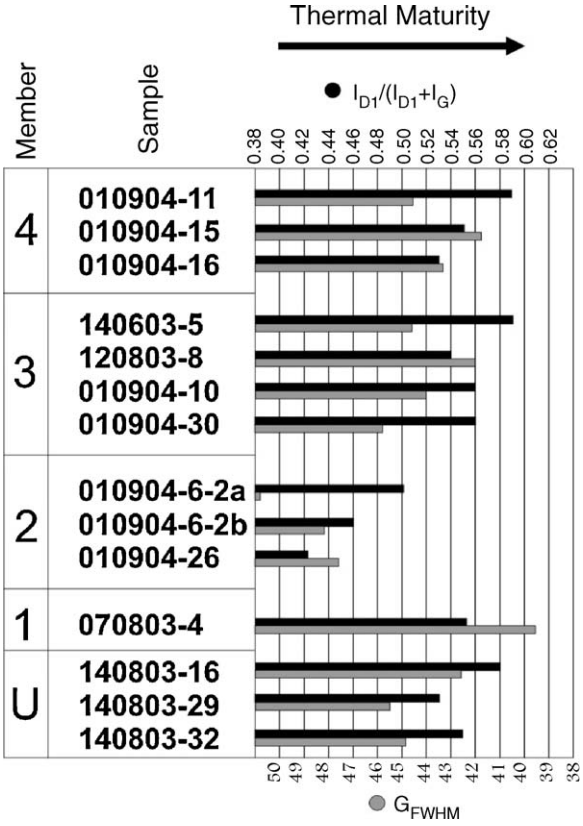

Fig. 6. Plot of $I_{D1}/(I_{D1}+I_G)$ and G_{FWHM} for each sample showing thermal maturity relationships with respect to sample locality. Samples from Member 2 show the lower degree of thermal maturity.

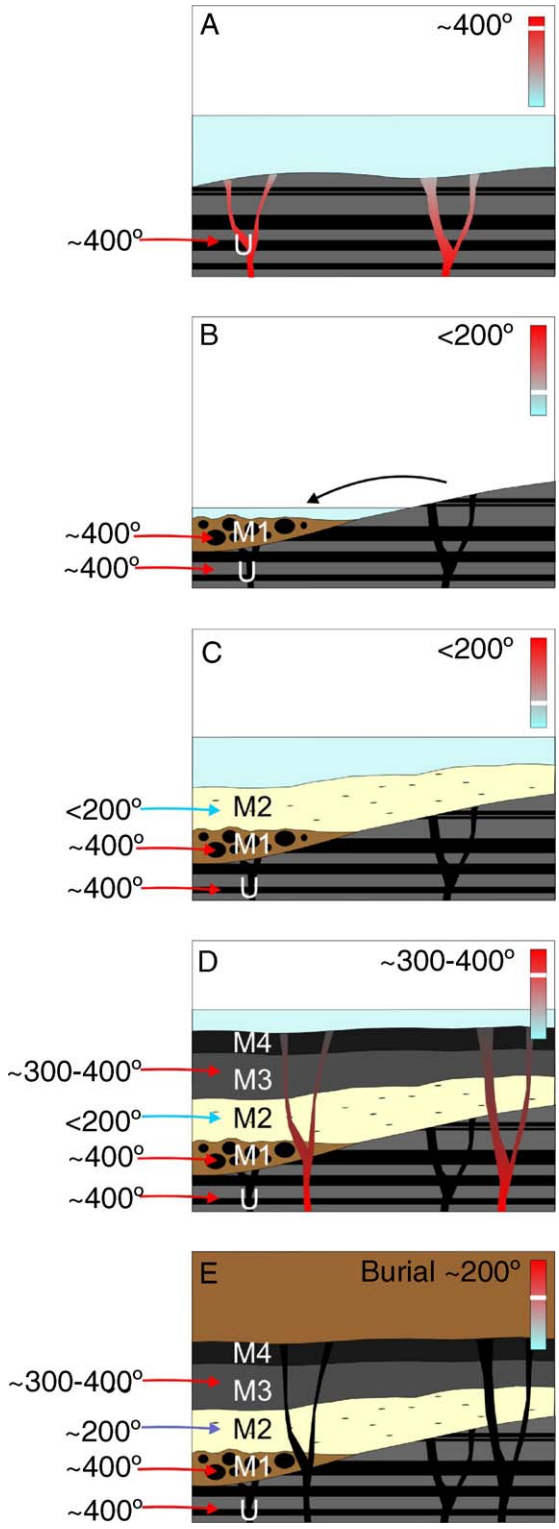

Fig. 7. Schematic diagram showing the reconstructed sequence of palaeoenvironments and thermal events that best explains the present day thermal maturity trends among carbonaceous materials in the Strelley Pool Chert. (A) Underlying rocks are deposited in a hot hydrothermal environment. (B) Underlying rocks are uplifted and eroded, depositing clasts of thermally mature carbonaceous chert in a cool shallow marine environment at the beginning of Strelley Pool Chert time. (C) Stromatolitic carbonate is deposited in a cool shallow marine environment. A small amount of carbonaceous material with low thermal maturity is preserved. (D) Member 3 and 4 are deposited in a hot environment (surface or near-surface temperatures,

mature samples (010904–11) comes from a hydrothermal black chert vein, as would be expected if original thermal signatures were preserved. The most convincing evidence lies in the contrasting thermal characteristics of CM in chert pebbles from Member 1 conglomerate (sample 070803–4) and CM in encrusting laminated carbonate immediately above the conglomerate (samples 010904-6-2a, 010904-6-2b). Field observations indicate that the encrusting carbonates were deposited immediately after the conglomerate and both conglomerate and carbonate would have been exposed to the same environments and post-burial thermal history [7–12]. However, spectra of CM in the pebbles have values for G_{FWHM}, $I_{D1}/I_G\sim$ and $I_{D1}/(I_{D1} + I_G)$ that indicate high thermal maturity that is comparable with the CM in the underlying strata from which the clasts were derived, whereas CM in encrusting carbonate have values that indicate the lowest thermal maturity in the entire sample suite. Evidently, the higher thermal maturity of the CM in the clasts was set by temperatures that occurred prior to deposition of Member 2 carbonates and that the carbonates never reached such high temperatures. Similarly, the thermal maturity of CM in the overlying Member 3 and Member 4 cherts must reflect the original hot depositional (or very early post-burial) environments of those cherts, which post-dated – and did not affect – Member 2. The present day thermal maturity of CM in the carbonate samples almost certainly reflects a post-depositional temperature to which the rocks were raised during burial, but that was still lower than the original palaeotemperatures of Member 3, 4 and underlying units (Fig. 7). This interpretation supports geological and geochemical indications of a hydrothermal environment of deposition for Member 3, Member 4 and underlying strata, and a (cooler) marine environment for the stromatolitic carbonates of Member 2 [7–12].

5. Conclusions

Syngenetic carbonaceous materials (CM) are preserved in sedimentary rocks of the Strelley Pool Chert, both in chert beds and in stromatolitic carbonate beds. The rocks have reached maximum temperatures of around 200–500 °C (reaching lower to mid Greenschist metamorphic facies) during their 3.43 billion-year history, as indicated by the Raman spectra of the CM. Within that temperature window, different layers and parts of the formation have reached different maximum temperatures, as indicated by small but distinct variations in the thermal maturity of CM. The variations are reflected in the Raman spectral characteristics of the CM and define thermal maturity trends that are linked to different strata and depositional facies. CM in rocks interpreted as hydrothermal in origin have higher thermal maturity than CM in rocks formed in a shallow marine environment [12]. This link between stratigraphic control on CM thermal maturity and other geological and geochemical indications of palaeoenvironmental change strongly suggests that the CM thermal maturity variations reflect original differences in the palaeoenvironments in which the carbonaceous sediments were deposited.

Thus, Raman spectral characteristics of CM in the Strelley Pool Chert provide important constraining evidence for palaeoenvironments and changes in environmental conditions through time. Moreover, Raman spectroscopy has shown that putative fossil stromatolites are not devoid of organic remains, and that the thermal treatment of CM in some rocks in the Strelley Pool Chert may have been sufficiently mild as to allow preservation of biomarker molecules (∼200 °C). Such rocks were quickly and easily identified using Raman spectroscopy, with geologic context providing constraints upon the primary nature of the signatures. This clearly demonstrates the usefulness of Raman spectroscopy in the search for microscopic traces of life on Earth, as well as on other planets or moons.

carbonates below remain cooler). The Strelley Pool Chert is buried for 3.43 billion years and reaches maximum burial temperatures of around 200 °C (at the study locality), probably raising the minimum thermal maturity of the CM in the area above original values.

Acknowledgements

Geological Survey of Western Australia and the Pilbara Regiment for field support; M. Van Kranendonk for assistance with Fig. 1; NSW Heritage Restoration Division for large sample cutting. Thank you also to E. Carter and the University of Sydney Vibrational Spectroscopy Unit. Research supported by Macquarie University and M.U. Biotechnology Research Institute. A.A. supported by Australian Postgraduate Award. CPM Acknowledges support from the Australian Research Council for funding and fellowship.

References

[1] F. Westall, J.N. Rouzaud, Geochim. Cosmochim. Acta Goldschmidt Conf. Abstr. (2004) A239.
[2] J.W. Schopf, A.B. Kudryavtsev, D.G. Agresti, T.J. Wdowiak, A.D. Czaja, Nature 416 (2002) 73.
[3] M.D. Brasier, O.R. Green, A.P. Jephcoat, A.T. Kleppe, M.J. Van Kranendonk, J.F. Lindsay, A. Steele, N.V. Grassineau, Nature 416 (2002) 76.
[4] B. Wopenka, J.D. Pasteris, Am. Mineral. 78 (1993) 533–557.
[5] C.P. Marshall, G.D. Love, C.E. Snape, A.C. Hill, A.C. Allwood, M.R.Walter, M.J. Van Kranendonk, R.E. Summons, Precam. Res., submitted for publication.
[6] M.J. Van Kranendonk, A.H. Hickman, R.H. Smithies, D.N. Nelson, G. Pike, Econ. Geol. 97 (2002) 695.
[7] A.C. Allwood, M.R. Walter, C.P. Marshall, M.J. Van Kranendonk, Int. J. Astrobiol. 3 (Supp. 1) (2004) 104.
[8] A.C. Allwood, M.R. Walter, C.P. Marshall, M.J. Van Kranendonk, Geol. Soc. Am. Abstr. Prog. (2004) 196.
[9] A.C. Allwood, M.R. Walter, M.J. Van Kranendonk, B.S. Kamber (2005) http://nai.arc.nasa.gov/nai2005/abstracts.cfm.
[10] A.C. Allwood, M.R. Walter, M.J. Van Kranendonk, B.S. Kamber (2005) http://nai.arc.nasa.gov/nai2005/abstracts.cfm.
[11] A.C. Allwood, M.R. Walter, M.J. Van Kranendonk, B.S. Kamber, European Geophysics Union Annual General Meeting Abstracts (2005).
[12] A.C. Allwood, M.R. Walter, B.S. Kamber, C.P. Marshall, I.W. Burch, Nature, in press.
[13] R. Buick, J.R. Thornett, N.J. McNaughton, J.B. Smith, M.E. Barley, M. Savage, Nature 375 (1995) 574.
[14] M.J. Van Kranendonk, Geol. Surv. Western Aust. 1:100,000. Geol. Series Explan. Notes, p. 86.

[15] A. Wang, P. Dhamelincourt, J. Dubessy, D. Guerard, P. Landais, M. Lelaurain, Carbon 27 (1989) 209.
[16] G. Katagiri, H. Ishida, A. Ishitani, Carbon (1988) 565.
[17] G. Compagini, O. Puglisi, G. Foti, Carbon 35 (1997) 1793.
[18] O. Beyssac, B. Goffe, J.-P. Petitet, E. Froigneux, M. Moreau, M.J.N. Rouzaud, Spectrochim. Acta A 59 (2003) 2267.
[19] F. Tuinstra, J.L. Koenig, J. Chem. Phys. 53 (1970) 1126.
[20] M.S. Dresselhaus, G. Dresselhaus, in: M. Cardona, G. Guntherodt (Eds.), Light Scattering in Solids III, Springer, Berlin, 1982, p. 187.
[21] M.J. Matthews, M.A. Pimenta, G. Dresselhaus, M.S. Dresselhaus, M. Endo, Phys. Rev. B 59 (1999) 6585.
[22] M.S. Dresselhaus, G. Dresselhaus, Adv. Phys. 30 (1981) 290.
[23] R. Al-Jishi, G. Dresselhaus, Phys. Rev. B 26 (1982) 4514.
[24] A. Cuesta, P. Dhamelincourt, J. Laureyns, A. Martinez-Alonso, J.M.D. Tascon, Carbon 32 (1994) 1523.
[25] T. Jawhari, A. Roid, J. Casado, Carbon 33 (1995) 1561.
[26] R.J. Nemanich, S.A. Solin, Phys. Rev. B 20 (1979) 392.
[27] C. Beny-Bassez, J.N. Rouzaud, Scan. Electron Micros. 1 (1985) 119.
[28] J. Jehlicka, O. Urban, J. Pokorny, Spectrochim. Acta A 59 (2003) 2341.
[29] F. Yui, E. Huang, J. Xu, J. Metamorph. Geol. 14 (1996) 115.
[30] K. Bucher, M. Frey, Petrogenesis of Metamorphic Rocks, Springer-Verlag, New York, 1994, p. 318.